

*Full Length Research Paper*

# Mechanochemical route to synthesize $\text{Co}_3\text{O}_4/\text{CuO}$ composite nanopowders

Aidong Tang<sup>1</sup>, Huaming Yang<sup>2,\*</sup>, Xiangchao Zhang<sup>2</sup>

<sup>1</sup> School of Chemistry and Chemical Engineering, Central South University, Changsha 410083, China; <sup>2</sup> School of Resources Processing and Bioengineering, Central South University, Changsha 410083, China

Accepted 17 October, 2006

$\text{Co}_3\text{O}_4/\text{CuO}$  composite nanopowders have been successfully synthesized by heating the precursor obtained via a mechanochemical reaction. The precursor and the nanopowders were characterized using thermogravimetric (TG), X-ray diffraction (XRD) and transmission electron spectroscopy (TEM). Subsequent thermal treatment of the precursor at 550-700 °C in air for 2 h resulted in the formation of  $\text{Co}_3\text{O}_4/\text{CuO}$  nanopowders with an average crystal size of about 25-50 nm, varying with the calcination temperature. The mechanism of nanocrystallite growth is primarily investigated. The morphology of the synthesized  $\text{Co}_3\text{O}_4/\text{CuO}$  nanopowders is in irregular polyhedron shape and the mechanism of NaCl used as diluent have been analyzed. The mechanochemical route is a novel, cheap and convenient technique suitable for large-scale synthesis of composite nanomaterials.

**Keywords:** Composite nanopowders;  $\text{Co}_3\text{O}_4/\text{CuO}$ ; Mechanochemical reaction; Nanocrystallite growth.

## INTRODUCTION

Transition metal oxides have been widely investigated due to their potential applications in many technological fields, such as catalysis, batteries, magnetic materials, gas sensor and solar energy conversion [Petitto and Langell, 2005; Radwan et al, 2003; Wojciechowska et al, 2006; Choi et al, 2004; Pillai and Deevi, 2006; Raveau, 2005; Gruyters, 2002; Wang et al 2004; Zaki, 2005; Wang et al, 2005]. Researches are being carried out to improve their efficiency to the maximum possible extent. Principally two strategies were adopted: changes in preparation methods and/or addition of another dopant [Radwan et al, 2003]. Mixed oxides of transition metals are capable of mutual interactions, leading to the formation of complex structure. The catalytic activity of mixed oxide systems is usually higher than that of their individual oxide components [Wojciechowska et al, 2006]. A great deal of fundamental research has been carried out on mixed oxides [Choi et al, 2004; Pillai and Deevi, 2006].

Cupric oxide (CuO), a narrow band-gap and p-type semiconductor, is an important material for a variety of

practical applications and cobalt oxide ( $\text{Co}_3\text{O}_4$ ), a spinel-type oxide and also p-type semiconductor, has very attractive electrocatalytic properties for many important reactions [Lia et al, 2005; Yin, et al. 2005].  $\text{Co}_3\text{O}_4$  and CuO nanoparticles have been respectively prepared by several methods and copper-cobalt-based catalysts (the spinel  $\text{CuCo}_2\text{O}_4$  and  $\text{Cu}_x\text{Co}_{3-x}\text{O}_4$ ) have been investigated [He et al, 2004; Ye et al, 1999; Singh et al, 2000.], but no report has focused on the preparation of  $\text{Co}_3\text{O}_4/\text{CuO}$  (p-p type) nanopowders. Mechanochemical processing is a novel method for the production of nanosized materials, where well-separated nanoparticles can be produced (Fores et al, 2001).

Recently, a wide variety of nanosized oxides have been synthesized by mechanochemical route, including CdO,  $\text{Co}_3\text{O}_4$ ,  $\text{CeO}_2$ ,  $\text{In}_2\text{O}_3$ ,  $\text{Cu}/\text{Al}_2\text{O}_3$  and  $\text{Fe}_2\text{O}_3/\text{SnO}_2$  [Yang et al, 2004; Lu and Fang, 2006; Hwang and Lee, 2005; Galatsis et al, 2003.]. Mechanochemical synthesis is particularly suitable for large-scale production because of its simple process and low cost. This paper first reports the synthesis of  $\text{Co}_3\text{O}_4/\text{CuO}$  composite nanopowders via mechano-chemical route.

\*Corresponding author. E-mail: [hmyang@mail.csu.edu.cn](mailto:hmyang@mail.csu.edu.cn); Tel: +86-731-8830549; fax: +86-731-871080.

## EXPERIMENTAL DETAILS

The starting materials were AR-grade  $\text{CoCl}_2 \cdot 6\text{H}_2\text{O}$ ,  $\text{CuCl}_2 \cdot 2\text{H}_2\text{O}$ ,

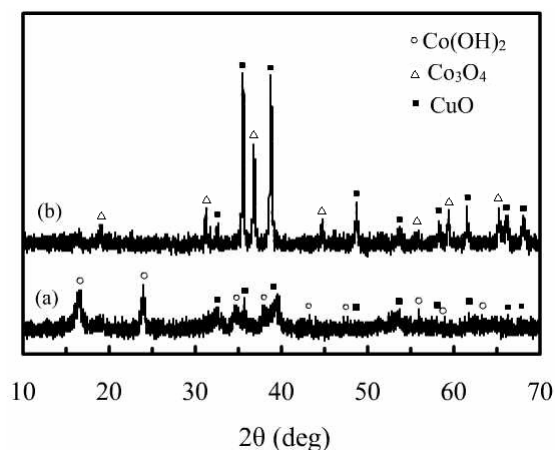


**Figure 1.** XRD patterns of the  $\text{InCl}_3 \cdot 4\text{H}_2\text{O} + \text{CuCl}_2 \cdot 2\text{H}_2\text{O} + \text{NaOH}$  powder mixture. (a) The precursor and (b) after calcination of the precursor at  $600^\circ\text{C}$  for 2h.

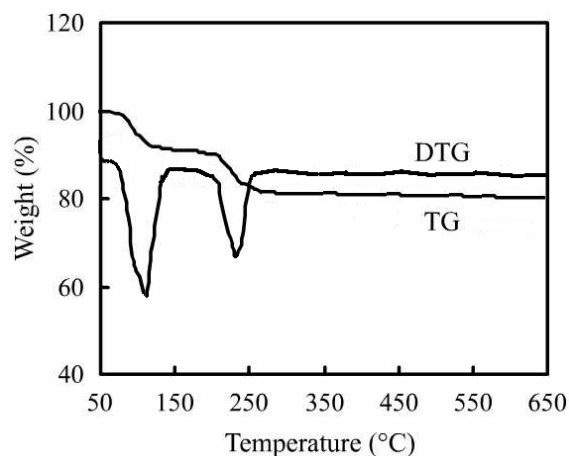


**Figure 2.** TG-DTG curves of the precursor.

$\text{NaOH}$  and  $\text{NaCl}$ .  $\text{NaCl}$  was used as a diluent and added to the starting powder. 70 wt.%  $\text{CuO}$  in the nanopowders is first determined in order to calculate the amount of the reactants. 5.00 g  $\text{CuCl}_2 \cdot 2\text{H}_2\text{O}$ , 2.96 g  $\text{CoCl}_2 \cdot 6\text{H}_2\text{O}$ , 3.34 g  $\text{NaOH}$  and 5.5 g  $\text{NaCl}$  were mixed and milled at ambient temperature in an agate mortar until the color of the as-milled powder kept unchanged. The reaction started immediately during the mixing process, accompanying the emission of water vapor from the system for exothermic effect of the reaction. Then the as-milled powder was dispersed in a 90W SK2200LH ultrasonic bath for 15 min, thoroughly washed with distilled water until no  $\text{Cl}^-$  anions could be detected in the solution with  $\text{AgNO}_3$  solution (0.10 mol/l) and dried at  $100^\circ\text{C}$  for 2 h in air to form the nanoparticle precursor. The precursor was heated at  $600^\circ\text{C}$  for 2 h in air in a porcelain crucible to form the black  $\text{Co}_3\text{O}_4/\text{CuO}$  nanopowders.

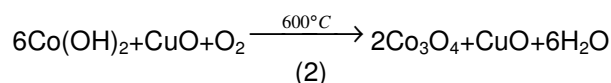
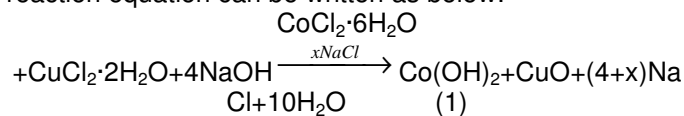
Thermogravimetric and differential thermogravimetric (TG/DTG) analysis of the precursor were performed in air atmosphere using a WCT-2 thermal analyzer with heating rate of  $10^\circ\text{C}/\text{min}$ . The precursor and nanopowders were examined by X-ray diffraction (XRD) (Rigaku, D/max- $\gamma\text{A}$ ,  $\text{CuK}\alpha$  radiation). The morphology of the

nanopowders was obtained using transmission electron microscopy (TEM, JEM-200CX), using an accelerating voltage of 200 kV. The average crystal size ( $D$ ) of the sample was calculated from the Scherrer's formula according to the half-width of the diffraction peak.

## RESULTS AND DISCUSSION

### Analysis of the synthesis reaction

During the mixing, the reaction was observed to be very fast, the color of the mixture changed frequently and remained black finally. Figure 1 shows the XRD patterns of the as-milled powders. After about 30min milling of the mixture and subsequently washed with distilled water, the  $\text{CuO}$  fine particles have been directly produced and the peaks of  $\text{Co}(\text{OH})_2$  are also evident. From the XRD profiles, it can be deduced that  $\text{CuO}$  is directly formed during the milling of the starting materials. Consequently, the solid-state diffusion is accelerated by the milling. Besides the  $\text{CuO}$  peaks, a new peak associated with  $\text{Co}_3\text{O}_4$  was observed in the pattern of the sample after calcination of the precursor at  $600^\circ\text{C}$  for 2 h, so the whole reaction equation can be written as below:



### TG-DTG analysis of the precursor

Figure 2 shows the TG-DTG curves of the precursor in air. There are two obvious endothermic peaks at about  $120^\circ\text{C}$  and  $240^\circ\text{C}$ , respectively. The first peak is attributed to the evaporation of surface water and the second one is due to the decomposition of structural water. It can be seen from the TG curve, there are two processes of the weight loss at about  $60\text{--}120^\circ\text{C}$  and  $200\text{--}250^\circ\text{C}$ , corresponding to 10.3% and 6.9% weight loss, respectively. It is interesting to find that the second weight loss (6.9%) is consistent with the calculated result (6.3%) of the separation of  $\text{H}_2\text{O}$  from the precursor  $\text{Co}(\text{OH})_2$ , which indicates that the second endothermic peak is corresponding to the decomposition of  $\text{Co}(\text{OH})_2$ . The results agree with those in XRD patterns of Figure 1.

### Morphology of nanopowders

Figure 3 shows the TEM image of the  $\text{Co}_3\text{O}_4/\text{CuO}$  nanopowders after calcination at  $700^\circ\text{C}$  in air for 2h. The average particle size of the as-prepared nanopowders is less than 50nm, which agrees well with the results that

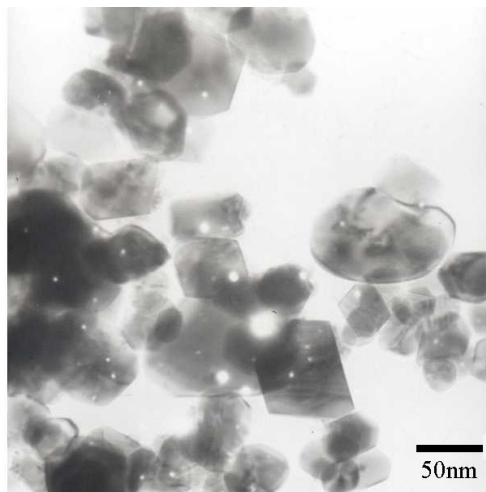


**Figure 3.** TEM images of the  $\text{Co}_3\text{O}_4/\text{CuO}$  nanopowders after calcination at  $700^\circ\text{C}$  in air for 2 h.

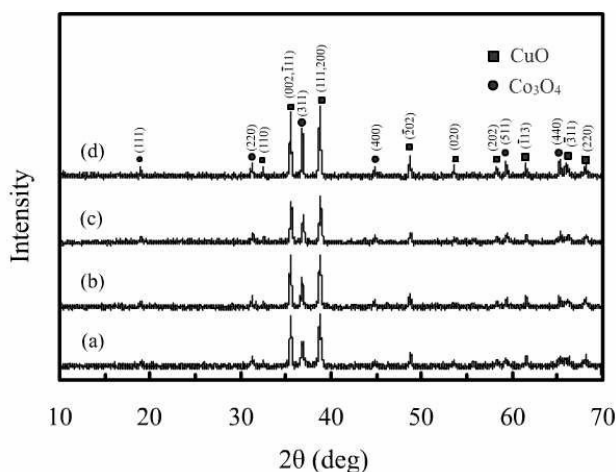


**Figure 4.** XRD patterns of  $\text{Co}_3\text{O}_4/\text{CuO}$  nanopowders at different calcination temperatures (a)  $550^\circ\text{C}$ ; (b)  $600^\circ\text{C}$ ; (c)  $650^\circ\text{C}$  and (d)  $700^\circ\text{C}$ .

are calculated based on XRD analysis. Figure 3 indicates that the  $\text{Co}_3\text{O}_4/\text{CuO}$  nanopowders are mainly in irregular polyhedron shape and well-dispersed. The irregular polyhedron shape of the nanopowders may be caused by the characters of the solid-state reaction, which can only take place on the interface of reactions. The growth of the nanoparticles varies in the different direction because the density and components are not homogeneous around the particles during the reaction (Thostenson et al, 2005).

### Effect of the calcination temperature

XRD patterns of the as-synthesized samples have been analyzed to investigate the phase structure in relation to

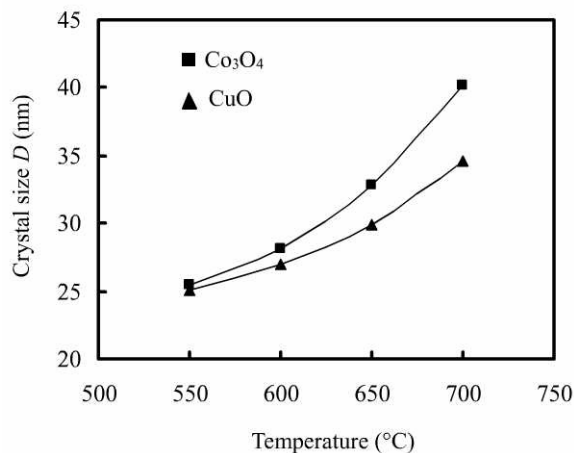


**Figure 5.** Effect of the calcination temperature on the average crystal size of  $\text{CuO}$  and  $\text{In}_2\text{O}_3$  of nanopowders.

the calcination temperature. Figure 4 shows the XRD patterns of  $\text{Co}_3\text{O}_4/\text{CuO}$  nanopowders after heat-treated at  $550\text{--}700^\circ\text{C}$  in air for 2 h. The results suggest that all the diffraction peaks can be readily indexed to the monoclinic structure of  $\text{CuO}$  in agreement with the literature (JCPDS 05-0661) and  $\text{Co}_3\text{O}_4$  with cubic structure (JCPDS 43-1003). The peak intensities of the  $\text{CuO}$  and  $\text{Co}_3\text{O}_4$  increased with increasing the calcination temperature, indicating a high degree of crystallization and the growth of nanocrystallites.

The average crystal sizes of the as-synthesized  $\text{Co}_3\text{O}_4/\text{CuO}$  nanopowders were calculated based on the Scherrer's formula. Figure 5 shows a plot of the XRD crystal size of  $\text{CuO}$  and  $\text{Co}_3\text{O}_4$  as a function of calcination temperature. The crystal size of  $\text{Co}_3\text{O}_4$  increased rapidly from about 25 nm at  $550^\circ\text{C}$  to 42 nm at  $700^\circ\text{C}$ , while that of  $\text{CuO}$  increased correspondingly slowly. The  $D$  values reach approximately 25 and 35 nm at  $550^\circ\text{C}$  and  $700^\circ\text{C}$ , respectively. This is directly related to the crystallization of nanoparticles. The result also indicates that the effect of the calcination temperature exists in the  $\text{Co}_3\text{O}_4/\text{CuO}$  composite nanopowders.

Straight lines of  $\ln D$  against  $1/T$  (Figure 6) are plotted according to the Scott equation given below under the condition of homogeneous growth of nanocrystallites, (Scott, 1983), which approximately describes the crystal growth during annealing:

$$D = C \exp(-E/RT) \quad (3)$$

where  $C$  is a constant,  $E$  is the activation energy,  $R$  is the gas constant, and  $T$  is the absolute temperature. There exists a good linear relationship. The  $E$  value was calculated from the slope of the straight line as  $E = 14.04$  kJ/mol and  $20.10$  kJ/mol for  $\text{CuO}$  and  $\text{Co}_3\text{O}_4$ , respectively. It shows that the calcination temperature

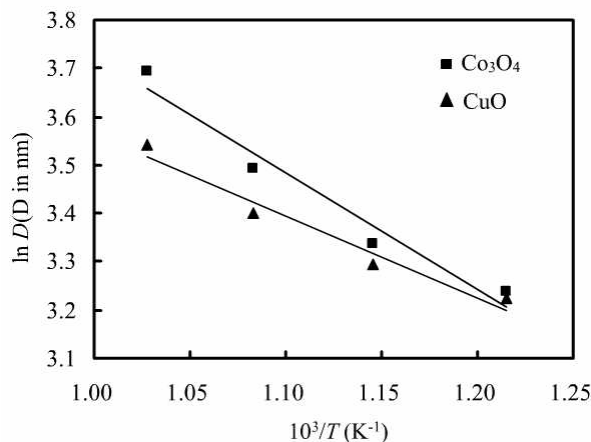


Figure 6. Plots of  $\ln D$  against  $1/T$  according to the Eq. (3).

has a more remarkable effect on the growth of nanocrystallites.  $\text{Co}_3\text{O}_4$  nanoparticles are a little more easily affected by thermal treatment than CuO, which can be observed from Figure 5.

### Mechanism of the diluent

In this experiment, NaCl is used as diluent during the process of preparation the  $\text{Co}_3\text{O}_4/\text{CuO}$  composite nanopowders. As shown in Figure 6, the individual particles are found to be well-dispersed without serious aggregates. This fact indicates that the presence of NaCl in the synthesized powder can inhibit particle agglomeration. Wiley and Kaner have suggested that the formation of salt provided an effective driving force for the formation of small particle (Yang et al, 2004). It can be concluded that the growth of the particles is inhibited by the addition of NaCl as diluent into the starting powder, due to the following reasons: (i) the formed NaCl tends to cover the reactant surface and hamper the further reaction, reducing the reaction volume between the reactant particles, leading to a decrease in reaction rate and the rate of heat generation; (ii) the diluent absorbs some of the collision energy during milling, reducing the energy transferring into the reactants, and (iii) the diluent absorbs heat generated by the reaction, reducing the temperature reached during milling. As a diluent material, NaCl has often been used because of its inert nature and excellent milling ability (Hwang and Lee, 2005). Recently, the influence of inert salts diluent on the morphology and particle size distribution of powders has attracted much attention because of many of its practical uses in synthesis of nanocrystalline particles with desirable characteristics, including very fine size, narrow size distribution, single crystal particle, high purity and good chemical homogeneity [Wiley and Kaner 1992; Li et al, 2005].

### CONCLUSIONS

Mechanochemical reaction of  $\text{CoCl}_2 \cdot 6\text{H}_2\text{O}$ ,  $\text{CuCl}_2 \cdot 2\text{H}_2\text{O}$  and NaOH resulted in the formation of a precursor during milling with NaCl as a diluent, which was then heated to produce  $\text{Co}_3\text{O}_4/\text{CuO}$  composite nanopowders. The morphology of the synthesized  $\text{Co}_3\text{O}_4/\text{CuO}$  nanopowders are in irregular polyhedron shape. The XRD crystal size of the  $\text{Co}_3\text{O}_4/\text{CuO}$  nanopowders rapidly increased with increasing calcination temperature. The crystal size varied from 25 to 50 nm at 550–700 °C. The activation energies of  $\text{Co}_3\text{O}_4/\text{CuO}$  nanocrystallite growth during thermal treatment were calculated to be 14.04 kJ/mol for CuO and 20.10 kJ/mol for  $\text{Co}_3\text{O}_4$ , respectively. The calcination temperature has a prominent effect on the nanocrystallite growth. The synthesized  $\text{Co}_3\text{O}_4/\text{CuO}$  nanopowders are promising for the advanced functional materials.

### ACKNOWLEDGEMENTS

This work was supported by the Program for New Century Excellent Talents in University (NCET-05-0695) and the Program for New Century 121 Excellent Talents in Hunan Province (05-030119).

### REFERENCES

- B. Raveau (2005). Transition metal oxides: Promising functional materials. *J. Eur. Ceram. Soc.* 25: 1965–1969.
- D Lia, YH Leunga, AB Djurisc (2005). CuO nanostructures prepared by a chemical method. *J. Cryst. Growth* 282: 105-111.
- ET Thostenson, C Li, TW Chou (2005). Nanocomposites in context, *Compos. Sci. Technol.* 65: 491-516.
- FH Fores, ON Senkov, EG Baburaj (2001). Synthesis of nanocrystalline materials an overview. *Mater. Sci. Eng. A* 301: 44-53.
- GX Wang, Y Chen, L Yang, J Yao, S Needham, HK Liu, JH Ahn (2005). Synthesis of nanocrystalline transition metal and oxides for lithium storage. *J. Power Sources.* 146: 487–491.
- HM Yang, YH Hu, XC Zhang (2004).  $\text{In}_2\text{O}_3$  nanoparticles synthesized by mechanochemical processing. *Scripta Mater.* 50: 413-415.
- J Lu, ZZ Fang (2006). Synthesis and characterization of nanoscaled Cerium (IV) oxide via a solid-state mechanochemical method. *J. Am. Ceram. Soc.* 89(3): 842-847.
- J Wang, S Uma, KJ Klabunde (2004). Visible light photocatalytic activities of transition metal oxide/silica aerogels. *Microporous Mesoporous Mater.* 75: 143–147.
- JB Wiley, RB Kaner (1992). Rapid solid-state precursor synthesis of materials. *Sci.* 255: 1093-1097
- K Galatsis, L Cukrov, W Wlodarski (2003). p- and n-type Fe-doped  $\text{SnO}_2$  gas sensors fabricated by the mechanochemical processing technique. *Sens. Actuators, B.* 93: 562-565.
- M Wojciechowska, M Zielinski, A Malczewska, W Przystajko, M Pietrowski (2006). Copper-cobalt oxide catalysts supported on  $\text{MgF}_2$  or  $\text{Al}_2\text{O}_3$ -their structure and catalytic performance. *Appl. Catal. A: General* 298: 225-231.
- M. Gruyters (2002). Structural and magnetic properties of transition metal oxide/metal bilayers prepared by in situ oxidation. *J. Magn. Magn. Mater.* 248: 248–257.
- M Yin, C Wu, Y Lou, C Burda, JT Koberstein, Yimei Zhu, Stephen O'Brien (2005). Copper oxide nanocrystals. *J. Am. Chem. Soc.* 127 (26): 9506-9511.

- MG Scott (1983). *Amorphous Metallic Alloys*, Butterworths, London. pp: 151.
- NRE Radwan, M Mokhtar, GA El-Shobaky (2003). Surface and catalytic properties of CuO and Co<sub>3</sub>O<sub>4</sub> solids as influenced by treatment with Co<sup>2+</sup> and Cu<sup>2+</sup> species. *Appl. Catal. A: General* 241: 77-90.
- RN Singh, JP Pandey, NK Singh (2000). Sol-gel derived spinel M<sub>x</sub>Co<sub>3-x</sub>O<sub>4</sub> (M=Ni,Cu; 0≤x≤1) films and oxygen evolution. *Electrochim. Acta* 45: 1911-1919.
- SC Petitto, MA Langell (2005). Cu<sub>2</sub>O (110) formation on Co<sub>3</sub>O<sub>4</sub> (110) induced by copper impurity segregation. *Surf. Sci.* 599: 27-40.
- SJ Hwang, J Lee (2005). Mechanochemical synthesis of Cu–Al<sub>2</sub>O<sub>3</sub> nanocomposites. *Mater. Sci. Eng. A.* 405: 140-146
- T He, DR Chen, XL Jiao (2004). Controlled Synthesis of Co<sub>3</sub>O<sub>4</sub> Nanoparticles through Oriented Aggregation. *Chem. Mater.* 16(4): 737-743.
- T Zaki (2005). Catalytic dehydration of ethanol using transition metal oxide catalysts. *J. Colloid Interface Sci.* 284: 606–613.
- UR Pillai, S Deevi (2006). Room temperature oxidation of carbon monoxide over copper oxide catalyst. *Appl. Catal. B: Environmental* 64: 146-151.
- US Choi, G Sakai, K Shimano, N Yamazoe (2004). Sensing properties of SnO<sub>2</sub>-Co<sub>3</sub>O<sub>4</sub> composites to CO and H<sub>2</sub>. *Sens. Actuators, B.* 98: 166–173.
- XR Ye, DZ Jia, JQ Yu, XQ Xin, ZL Xue (1999). One-step solid-state reactions at ambient temperatures-a novel approach to nanocrystal synthesis. *J. Adv. Mater.* 11(11): 941-942.
- YX Li, WF Chen, XZ Zhou (2005). Synthesis of CeO<sub>2</sub> nanoparticles by mechanochemical processing and the inhibiting action of NaCl on particle agglomeration. *Mater. Lett.* 59: 48-52.